

ACCEPTED MANUSCRIPT

## Tuning dimensionality in van-der-Waals antiferromagnetic Mott insulators $\text{TMPS}_3$

To cite this article before publication: Matthew John Coak *et al* 2019 *J. Phys.: Condens. Matter* in press <https://doi.org/10.1088/1361-648X/ab5be8>

### Manuscript version: Accepted Manuscript

Accepted Manuscript is “the version of the article accepted for publication including all changes made as a result of the peer review process, and which may also include the addition to the article by IOP Publishing of a header, an article ID, a cover sheet and/or an ‘Accepted Manuscript’ watermark, but excluding any other editing, typesetting or other changes made by IOP Publishing and/or its licensors”

This Accepted Manuscript is © 2019 IOP Publishing Ltd.

During the embargo period (the 12 month period from the publication of the Version of Record of this article), the Accepted Manuscript is fully protected by copyright and cannot be reused or reposted elsewhere.

As the Version of Record of this article is going to be / has been published on a subscription basis, this Accepted Manuscript is available for reuse under a CC BY-NC-ND 3.0 licence after the 12 month embargo period.

After the embargo period, everyone is permitted to use copy and redistribute this article for non-commercial purposes only, provided that they adhere to all the terms of the licence <https://creativecommons.org/licenses/by-nc-nd/3.0>

Although reasonable endeavours have been taken to obtain all necessary permissions from third parties to include their copyrighted content within this article, their full citation and copyright line may not be present in this Accepted Manuscript version. Before using any content from this article, please refer to the Version of Record on IOPscience once published for full citation and copyright details, as permissions will likely be required. All third party content is fully copyright protected, unless specifically stated otherwise in the figure caption in the Version of Record.

View the [article online](#) for updates and enhancements.

# Tuning dimensionality in van-der-Waals antiferromagnetic Mott insulators $TMPS_3$

M.J. Coak,<sup>1</sup> D.M. Jarvis,<sup>2</sup> H. Hamidov,<sup>2,3,4</sup> C.R.S. Haines,<sup>5</sup> P.L. Alireza,<sup>2</sup> C. Liu,<sup>2</sup> Suhan Son,<sup>6,7</sup> Inho Hwang,<sup>6,7</sup>  
G.I. Lampronti,<sup>5</sup> D. Daisenberger,<sup>8</sup> P. Nahai-Williamson,<sup>2</sup> A.R. Wildes,<sup>9</sup> S.S. Saxena,<sup>2,4</sup> and Je-Geun Park<sup>6,7</sup>

<sup>1</sup>Department of Physics, University of Warwick, Gibbet Hill Road, Coventry CV4 7AL, UK

<sup>2</sup>Cavendish Laboratory, Cambridge University, J.J. Thomson Ave, Cambridge CB3 0HE, UK

<sup>3</sup>Navoi State Mining Institute, 27 Galaba Avenue, Navoi, Uzbekistan

<sup>4</sup>National University of Science and Technology "MISiS", Leninsky Prospekt 4, Moscow 119049, Russia

<sup>5</sup>Department of Earth Sciences, Cambridge University, Downing Street, Cambridge CB2 3EQ, UK

<sup>6</sup>Center for Correlated Electron Systems, Institute for Basic Science, Seoul 08826, Republic of Korea

<sup>7</sup>Department of Physics and Astronomy, Seoul National University, Seoul 08826, Republic of Korea

<sup>8</sup>Diamond Light Source, Chilton, Didcot OX11 0DE, UK

<sup>9</sup>Institut Laue-Langevin, 6 rue Jules Horowitz, BP 156, 38042 Grenoble Cedex 9, France

(Dated: November 12, 2019)

We present an overview of our recent work in tuning and controlling the structural, magnetic and electronic dimensionality of 2D van-der-Waals antiferromagnetic compounds (Transition-Metal)PS<sub>3</sub>. Low-dimensional magnetic systems such as these provide rich opportunities for studying new physics and the evolution of established behaviours with changing dimensionality. These materials can be exfoliated to monolayer thickness and easily stacked and combined into functional heterostructures. Alternatively, the application of hydrostatic pressure can be used to controllably close the van-der-Waals interplanar gap and tune the crystal structure and electron exchange paths towards a 3D nature. We collect and discuss trends and contrasts in our data from electrical transport, Raman scattering and synchrotron x-ray measurements, as well as insight from theoretical calculations and other results from the literature. We discuss structural transitions with pressure common to all materials measured, and link these to Mott insulator-transitions in these compounds at high pressures. Key new results include magnetotransport and resistivity data in the high-pressure metallic states, which show potentially interesting qualities for a new direction of future work focussed on low temperature transport and quantum critical physics.

Dimensionality is crucial in determining or controlling the magnetic, electronic and structural properties of condensed matter systems. The case of 2D and of graphene is of course a very topical example. The pairing mechanisms of unconventional superconductors such as high-temperature superconductors and FeSe are often seen to be strengthened in 2D. Additionally, new magnetic phases and structures can be found in thin films or layers of otherwise simplistic materials. Crystals with layered structures of atomic planes separated by van-der-Waals gaps form an ideal case for studying a wide range of phenomena in the 2D limit [1–5], and how phases and interactions evolve as we then tune that system towards 3D or conversely reduce the thickness to single atomic layers.

A very mature and established line of research into van-der-Waals (vdW) physics has for some time focussed on the transition-metal-dichalcogenides (TMDs) [6]. New options and classes of materials are however essential for both the designers of a new generation of 2D functional devices and fundamental physics researchers. The  $TMPS_3$  family of compounds, with  $TM$  a first-row transition metal, has in contrast until recently received little scrutiny, despite being originally discovered in the 1890's and carefully characterised in the 1980's [7–14]. These materials bring both magnetism and correlated electron physics to the playground of vdW materials - reviews can be found at Refs [15–19]. They all share

the same basic crystal structure, shown in Fig 1 - a  $C2/m$  monoclinic cell with a honeycomb arrangement of metal ions. These metal ions, the magnetic sites, form very close to ideal hexagons in the  $ab$  plane, separated by wide vdW gaps with weak bonds and interactions along the perpendicular  $c^*$  axis. Covalent  $P_2S_6$  clusters surround the honeycombs, and mediate both the interplanar interactions and in-plane superexchange. There has been significant study into the magnetism and magnetic structures of this family [20–35], as these materials form a rich playground for investigating fundamental low-dimensional magnetism. Altering the choice of metal ion can give rise to Ising-type, XY or Heisenberg antiferromagnetic magnetic order, different spin states, including non-magnetic references like  $ZnPS_3$ , and subtly differing exchange interaction strengths. These lead to a wide selection of magnetic structures and interactions, some of which are displayed in Fig 1. Intermediate compounds can also be grown through the same simple chemical vapour transport method as the parent compounds -  $CuInP_2S_6$  is ferroelectric [36–39] and  $MnFeP_2S_6$  exhibits spin-glass behaviour due to the competing Ising and Heisenberg nature of the Fe and Mn magnetic sites [40, 41]. These mixed compounds promise a further rich future research direction beyond tuning and studying the 'pure' compounds discussed in this work.

The transport properties of  $TMPS_3$  materials also exhibit fascinating correlated electron physics. Many of

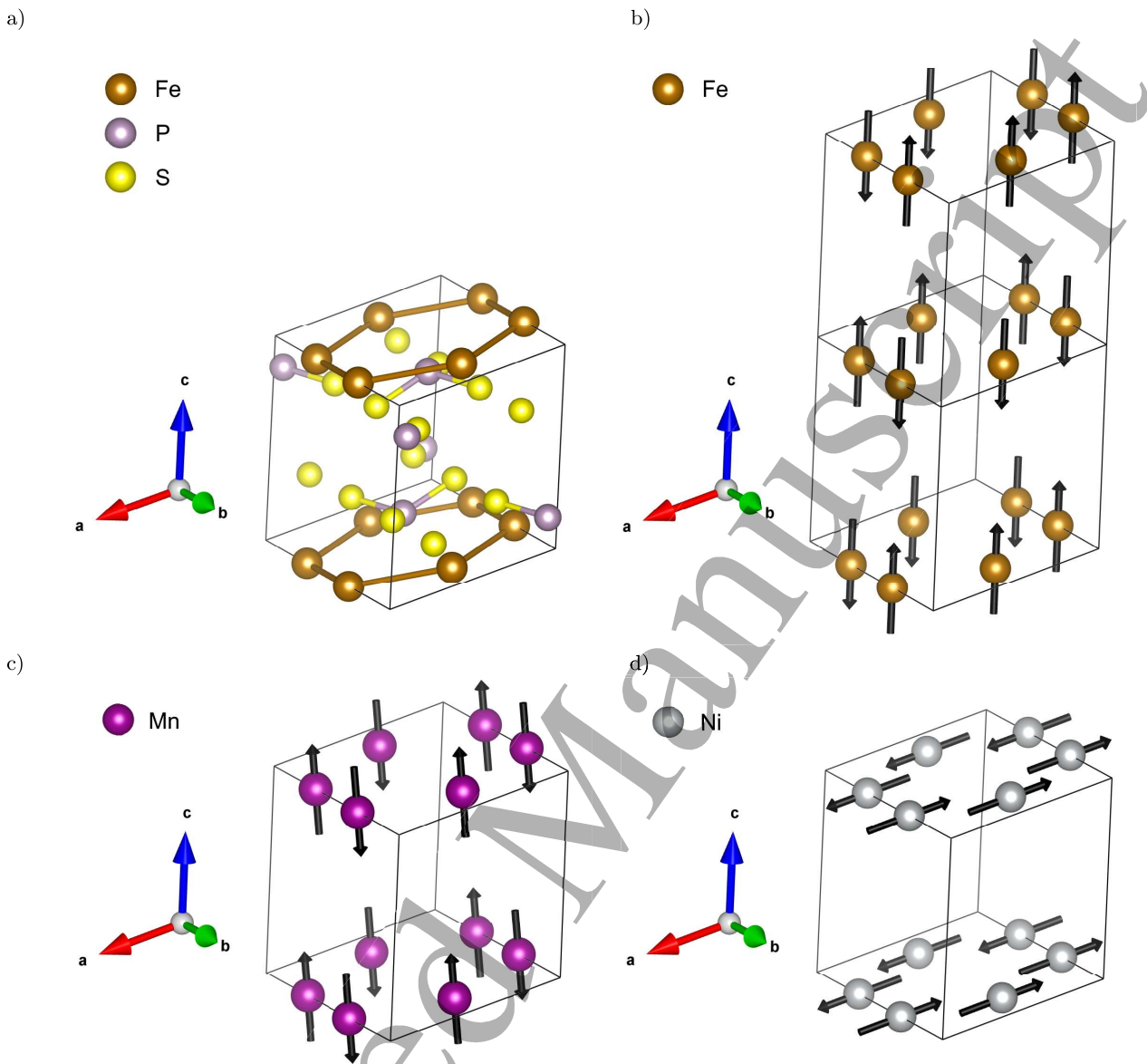


FIG. 1. Crystal and magnetic structures of FePS<sub>3</sub>, MnPS<sub>3</sub> and NiPS<sub>3</sub>. Fe atoms are pictured in brown, Ni in grey, Mn in dark purple, P in lilac and S in yellow. P and S atoms are omitted from the magnetic structure diagrams. a) Crystal structure of ambient pressure FePS<sub>3</sub> [13]. b) Magnetic structure of FePS<sub>3</sub> - Ising spins directed along  $c^*$  forming chains along  $a$  with AFM coupling between them in- and out-of-plane, propagation vector  $[0\ 1\ 1/2]$  [34]. c) Magnetic structure of MnPS<sub>3</sub> - Heisenberg spins canted  $8^\circ$  from  $c^*$  forming AFM chains, propagation vector  $[0\ 0\ 0]$  [28, 42]. d) Magnetic structure of NiPS<sub>3</sub> (and CoPS<sub>3</sub>)- Ising spins directed long  $a$  forming chains along  $a$  with AFM coupling between them in-plane, FM out-of-plane, propagation vector  $[0\ 1\ 0]$  [33].

these materials are Mott or Charge-Transfer insulators, with a wide range of electronic band gaps exhibited, from 0.25 eV in  $V_x\text{PS}_3$  [13] to 3.5 eV in  $\text{ZnPS}_3$  [19, 43, 44]. The characteristics and influence of the sulphur bonds and chemistry, in contrast to the well-trodden ground of oxide physics, is an additional avenue of interest in these materials. A 2D antiferromagnetic Mott insulator state, as found in these compounds, has great appeal for the study of fundamental correlated electron physics, par-

ticularly the behaviour as such a state is suppressed or tuned towards a phase transition - many high- $T_c$  superconductors emerge from just such a state for example. Indeed, the selenium analogue  $\text{FePSe}_3$  has recently been found to become superconducting at high pressures [45].

As showcased in Fig 2, a major advantage of the  $\text{TMPS}_3$  materials is that they can be easily and cleanly exfoliated into controllably thin layers by use of the now-famous 'Scotch tape' method [46]- and they remain air-

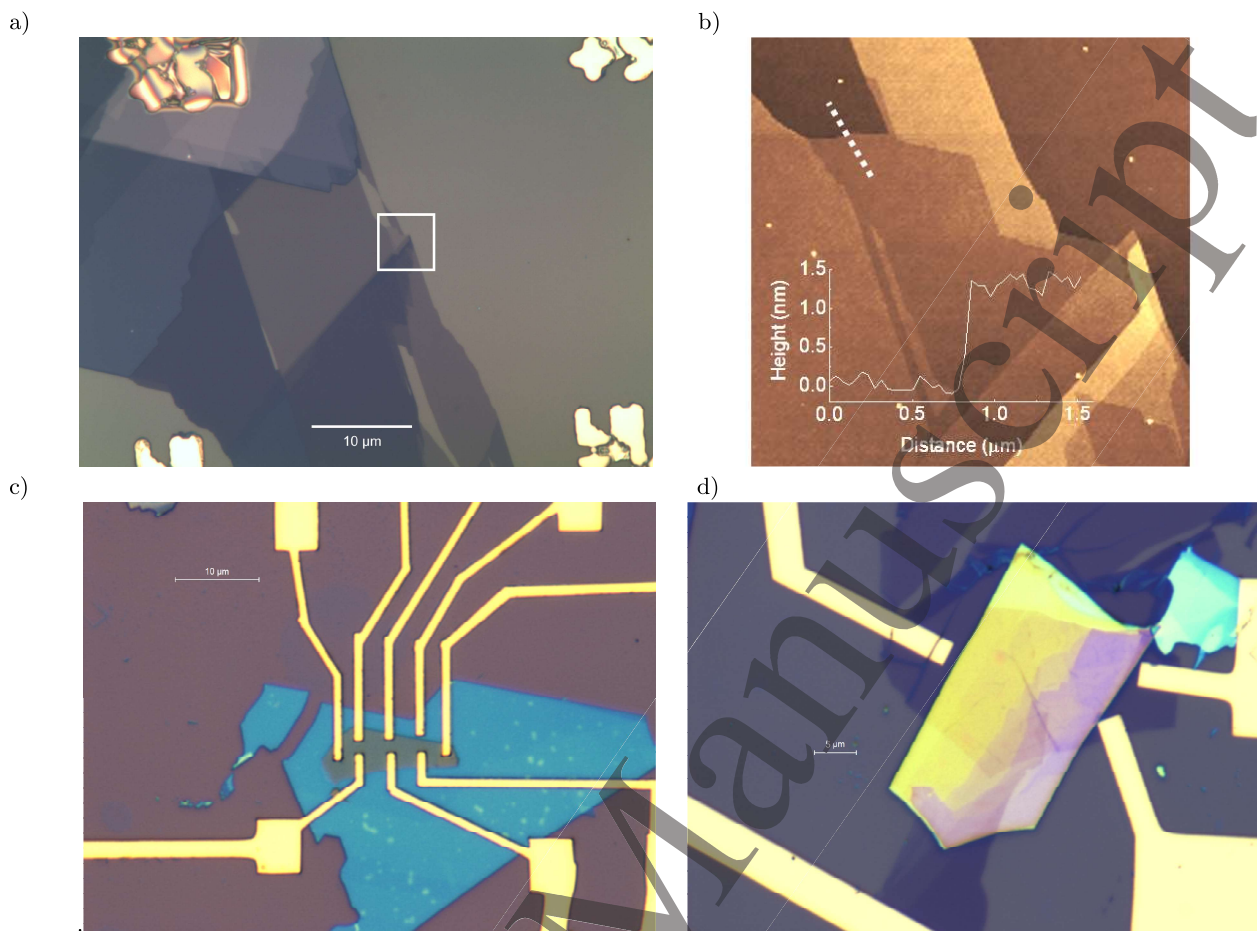


FIG. 2. Examples of  $TMPS_3$  exfoliated flakes and devices assembled by mechanical exfoliation and dry transfer techniques on Si/SiO<sub>2</sub> substrates. a) An exfoliated flake of NiPS<sub>3</sub>, exhibiting a selection of thicknesses and hence colours. b) AFM topography image and line profile (along dotted white line) from the boxed region in (a). The 1.3 nm observed height of a single 0.5 nm layer is due to the gap between sample and substrate - verified by observing a bilayer at 1.8 nm. c) Hall bar device assembled from an FePS<sub>3</sub> / Fe<sub>3</sub>GeTe<sub>2</sub> heterostructure. d) a graphene - CuInP<sub>2</sub>S<sub>6</sub> - graphene heterostructure, with graphene acting as contact electrodes to allow capacitance measurements of very thin samples of this ferroelectric material.

and moisture-stable. This allows detailed thickness dependence studies of the magnetism, vibrational and optical properties and transport, down to single monolayers. Recent work [47] was able to clearly demonstrate the prediction of Onsager that Ising-type magnetic order can remain stable at the 2D limit by studying the Raman spectra of FePS<sub>3</sub> with varying sample thickness and temperature. Further studies [48, 49] were able to show the suppression of XXZ-type order in NiPS<sub>3</sub> in the monolayer limit, as well as the loss of order in Heisenberg MnPS<sub>3</sub> in single layers - but interestingly the order survives down to bilayer thickness. As well as magnetism, members of this family such as CuInP<sub>2</sub>S<sub>6</sub> display order of electric polarisation - there is potential to cleanly investigate ferroelectricity, the often-neglected analogue of ferromagnetism, down to 2D thicknesses. Additionally, flakes of these materials can be picked up and stacked through a dry-transfer technique to form functional het-

erostructures [5, 50] combining or placing in competition the properties of the constituent layers and preserving clean interfaces between them.

While exfoliation varies the dimensionality of the system between quasi-2D and true-2D, applying hydrostatic pressure has an effect we can view as essentially opposite - the system will be tuned towards three dimensionality. As the vdW forces between planes are so much weaker than intra-planar interactions, the effect of hydrostatic pressure will overwhelmingly be to push the crystal planes together (and a dramatic effect from even small pressures can be expected), until eventually the vdW gap is closed and bonds form between the planes. As pressure can be continuously and controllably varied, it forms a finer and cleaner tuning parameter than chemical doping or thickness control. In the following sections we outline and discuss our recent results from measurements of structure, optical properties and electrical transport in

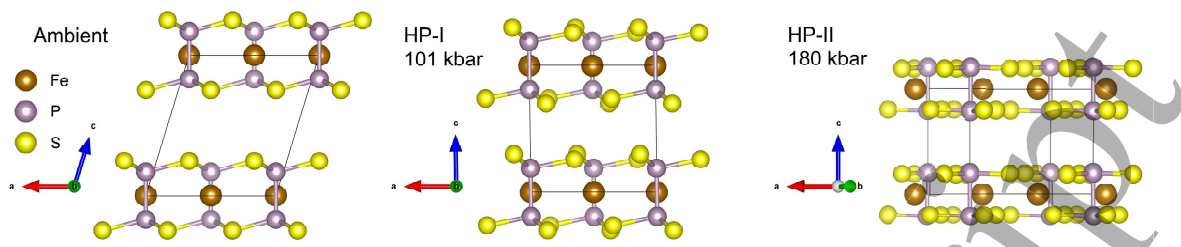


FIG. 3. Ambient-pressure and the two high-pressure structural phases of  $\text{FePS}_3$ , based on structural data from Ref [51]. The three structures are drawn to the same scale for comparison.

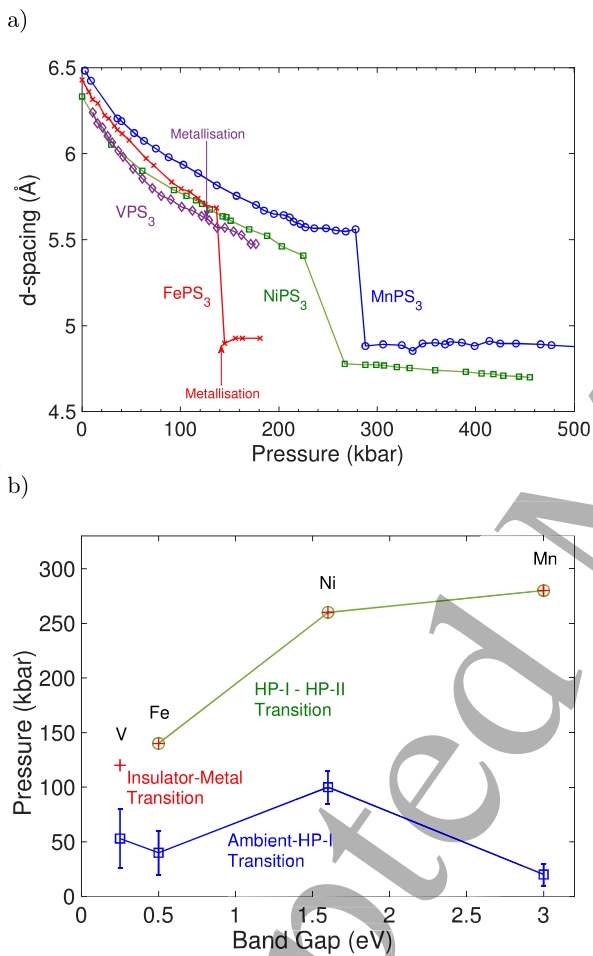


FIG. 4. a) Interplanar  $c^*$   $d$ -spacing of  $\text{TMPS}_3$  ( $\text{TM} = \text{V}, \text{Fe}, \text{Mn}, \text{Ni}$ ) plotted against pressure at room temperature, from Refs [51–53]. This corresponds to the interplanar distance, independent of the symmetry or unit cell model used. A sharp collapse seen in all but the V compound (so far) corresponds to the HP-I to HP-II structural transition. b) Transition pressures of these compounds at room temperature plotted against their ambient pressure band gaps. In  $\text{V}_{0.9}\text{PS}_3$  alone does the insulator-metal transition not correspond to the HP-I to HP-II volume collapse. This transition has not yet been observed in this vanadium compound - data were taken up to 180 kbar.

diamond anvil pressure cells, as described in Refs [51–54].

We measured the dependence of the crystal structure upon pressure in  $\text{FePS}_3$ ,  $\text{V}_{0.9}\text{PS}_3$ ,  $\text{MnPS}_3$  and  $\text{NiPS}_3$  within diamond anvil cells with helium pressure media and at room temperature in a series of powder diffraction experiments at the Diamond Light Source. The significant preferred orientation present in powders of these layered materials makes extracting a crystal structure solution from a powder pattern challenging - for example the (001) diffraction peak is not seen in some previous experiments [45, 55], despite being the most dominant peak in a theoretical perfectly randomly oriented powder. Without an accurate determination of the position of the (001) peak it is all but impossible to formulate a reliable structural model. Through careful preparation of the sample powder and rocking of the sample during data collection, our measurements were able to clearly resolve this peak, though it remains weak [51, 52]. The position of the (001), and hence the magnitude of  $c^*$ , directly tells us the inter-planar spacing, the most crucial parameter in the dimensionality tuning. Information on the correct crystal structures and their evolution is critical to inform any ab-initio theoretical calculations to explore the physics in these systems further.

In all the compounds measured to date, a pair of subsequent structural transitions (Fig 3) are seen to occur as pressure is increased, seemingly common to the whole isostructural family. Taking the shown example of  $\text{FePS}_3$ , the first transition from the ambient structure [13] to what we denote the HP-I phase corresponds to a shear of the crystal planes along the  $a$  axis. This preserves the same monoclinic space group but brings the  $\beta$  angle very close to 90 degrees and so metal ions, and the exchange ligands, now sit directly above their neighbours in the adjacent plane. This can be expected to have an impact on the magnetic inter-planer order as well as electron hopping. This transition does not include a volume change of the unit cell and is seen to evolve over a surprisingly wide pressure range, with a phase coexistence of the ambient and HP-I phases over the regions shown by error bars in Fig 4.b. As shown in this figure, there appears to be no correlation between the electronic band

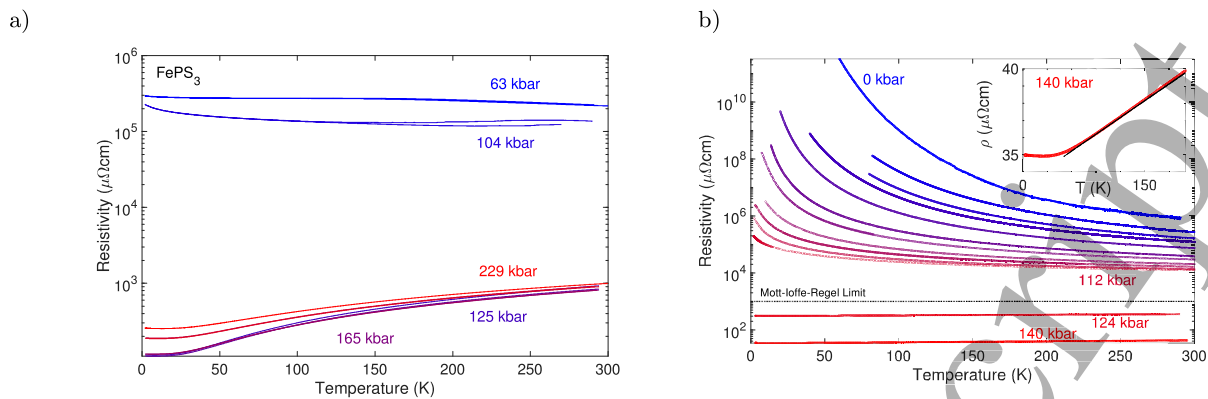


FIG. 5. Insulator-metal transitions in a)  $\text{FePS}_3$  and b)  $\text{V}_{0.9}\text{PS}_3$  [52]. Both show Kondo-like upturns at low temperature. In the V compound, the resistivity appears linear in  $T$ , except for the upturn, but such a relation does not appear to hold for  $\text{FePS}_3$ .

gap, insulator-metal transition pressure or second transition pressure and this first transition's pressure value. However, as outlined in Brec's review [16], both the P-P bond lengths and cation ionic radius increase in the sequence Ni-V-Fe-Mn in the  $\text{TMPS}_3$  compounds, just as the ambient-HP-I transition pressure, hinting that these properties may be responsible for determining the transition pressure. The case of  $\text{CdPS}_3$  is additionally an interesting one - Lifshitz et al. [56] and then Boucher et al. [57] previously reported a seemingly equivalent transition to a 90 degree  $\beta$ , reportedly trigonal, space group upon lowering temperature below 228 K, with a similar phase mixing behaviour - an interesting future direction may be to explore the full pressure-temperature structural phase diagrams of these materials.

The second transition, at higher pressures, is a significant collapse of the  $c^*$  interplanar spacing - clear in the (001)  $d$ -spacings shown in Fig 4.a. This is accompanied by a change in symmetry and unit cell - in  $\text{FePS}_3$  to a trigonal  $P-31m$  trigonal space group. This transition was not observed in the vanadium compound up to the maximum measured pressure of 180 kbar, despite this compound having the lowest band gap and resistivity. This HP-I to HP-II transition corresponds to a reduction of unit cell volume by up to 20%, appears to occur sharply, and has a large pressure hysteresis - the material remains in the HP-II phase even when nearly all the load is removed from the cell, suggesting a strong first-order nature. Such a dramatic change in the structure can certainly be expected to manifest in changes to the magnetism and transport, and indeed in Fe, Mn and  $\text{NiPS}_3$  we can associate the insulator-metal transition pressure with this structural transition.

All of the  $\text{TMPS}_3$  compounds measured thus far have exhibited some form of insulator (semiconductor) to metal transition at elevated pressures [45, 51, 52, 55, 58, 59] - examples for the cases of  $\text{FePS}_3$  and  $\text{V}_{0.9}\text{PS}_3$  are shown in Fig 5. The vanadium compound shows a

unique difference from the rest of the family - as displayed in Fig 4.b, in all other materials measured the insulator-metal transition occurs coincident with the HP-I to HP-II structural phase transition. Such a significant collapse of the unit cell will bring interplanar separation of, for instance, the P atoms down to a length where electron overlap and bond formation can be expected - a 3D character and movement of electrons between planes and sites is then unsurprising. Extra bond formation is also consistent with valence changes upon metallisation reported by Wang et al. In  $\text{V}_{0.9}\text{PS}_3$  however, metallisation is observed to occur gradually and smoothly, in the absence of any structural change [52].  $\text{V}_{0.9}\text{PS}_3$ , unlike the other materials, also shows variable-range-hopping type resistivity (with a pressure-dependent Arrhenius-type exponent), rather than conventional Arrhenius-type activated exponential insulating resistivity.

An additional interesting difference between these two cases is the temperature dependence of the resistivity  $\rho$  in the high-pressure metallic states. Both show the previously reported resistivity upturns at low temperature - Kondo-like but not fully explained at this time. Above the upturn temperature, metallic  $\text{V}_{0.9}\text{PS}_3$  exhibits linear  $\rho$  vs  $T$  as may be expected for a highly disordered system at elevated temperatures - the residual resistance ratio (RRR,  $\rho(300\text{K})/\rho(2\text{K})$ ) is additionally very small at around 1.2.  $\text{FePS}_3$  in contrast has a RRR of around 8, and a temperature dependence which appears to deviate from a linear or quadratic relation - a hint that a potential future direction for research into these systems may be non-Fermi-liquid or quantum critical physics in the high-pressure 'strange metal' states.

The magnetoresistance at low temperature of these two compounds additionally displays striking contrasts. As shown in Fig. 6, which plots fractional magnetoresistance - the field-symmetric component of  $\rho(B)$  normalised as  $(\rho_{sym}(B) - \rho(0)) / \rho(0)$  and plotted as a percentage, the  $\rho(B)$  dependences are very different between  $\text{V}_{0.9}\text{PS}_3$  and

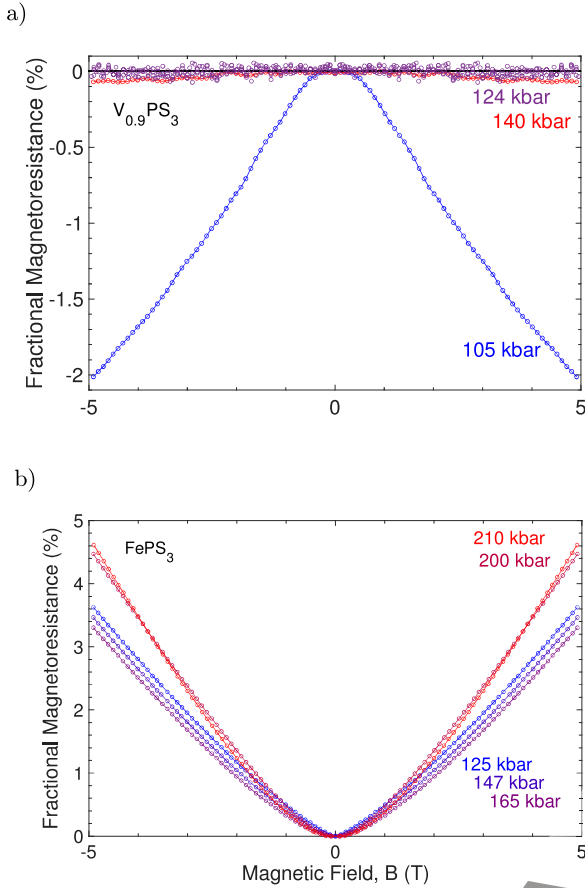


FIG. 6. Magnetoresistance of V and  $FePS_3$  at 2 K at increasing pressures. a) Fractional magnetoresistance, FMR,  $(\rho_{sym}(B) - \rho(0)) / \rho(0)$  of  $V_{0.9}PS_3$  at 2 K, above and below the metallisation pressure of 120 kbar (all in the HP-I phase). b) FMR of  $FePS_3$  at 2 K, at high pressures in the metallic HP-II phase.

$FePS_3$ . In the insulating state of  $V_{0.9}PS_3$  at 105 kbar, just before the insulator-metal transition, the magnetoresistance is linear in field (except at very small fields) and negative - increasing the magnetic field lowers the resistance at 2 K. After passing through the transition however, the magnetoresistance effect is then absent or very small. Due to the significantly higher resistance, we were not able to measure low-temperature magnetoresistance in the HP-I state of  $FePS_3$ , but the metallic state above 120 kbar shows a significant positive magnetoresistance, in contrast to the vanadium case.

A final example is the study of high-pressure Raman spectra - again, complementary to the thickness-dependent Raman studies. In a recent paper [54] we were able to track the evolution of the Raman spectrum of room-temperature  $V_{0.9}PS_3$  with pressure, through the transition to the HP-I structural phase and the insulator-metal transition. We additionally were able to carry out ab-initio calculations of high-pressure phonon modes and

band structure, for the first time using the detailed structural data from the high-pressure measurements. Visualisations of two of the vibrational modes assigned to two of the key peaks are shown in Fig 7. A key result is that peak p2 - and only p2 - stiffens significantly at the insulator-metal transition. This mode is uniquely and specifically a motion along the interplanar  $c'$  direction, so this stiffening supports the increase in electron cloud dimensionality suggested by the transport data in this material - the very tuning from 2D to 3D we desire to study.

## DISCUSSION

We have presented an overview of our recent progress on investigating the effect of tuning dimensionality on the structural and transport properties of Mott insulating layered  $TMPS_3$  materials. These compounds offer a rich variety of electronic and magnetic states to study the evolution of, and can be tuned through thickness control, chemical doping or hydrostatic pressure from truly 2D up to a 3D structure by merit of their weak van-der-Waals interplanar interactions. The presence of both antiferromagnetism and the strong electron correlations and Mott physics in these materials - which can be cleanly controlled via pressure - offer new avenues to explore in 2D and device physics.

Two structural transitions are found to be common to the family - a shear of the planes, here argued to occur at pressures scaling with metal ion radius, and then a collapse of the interplanar spacing and a raising of the crystal symmetry. In all cases except the vanadium compound, which forms an interesting exception, an insulator-metal Mott transition accompanies this strongly first-order second transition, and the pressure value of this scales with ambient-pressure energy gap. Ab-initio theoretical calculations using the structures discovered from pressure measurements show agreement with the observed transport and vibrational data, and have begun to give insight into the links between dimensionality and the phonon modes in these compounds. A detailed pressure dependence of the structural parameters and symmetries is essential to inform future theoretical studies and predictions. Both the resistivity and magnetoresistance of metallic high-pressure  $FePS_3$  and  $V_{0.9}PS_3$  were observed to show key differences and several effects remain to be investigated or explained. Detailed study of the potentially unconventional metallic states in these high pressure phases shows promise as a future direction in this field.

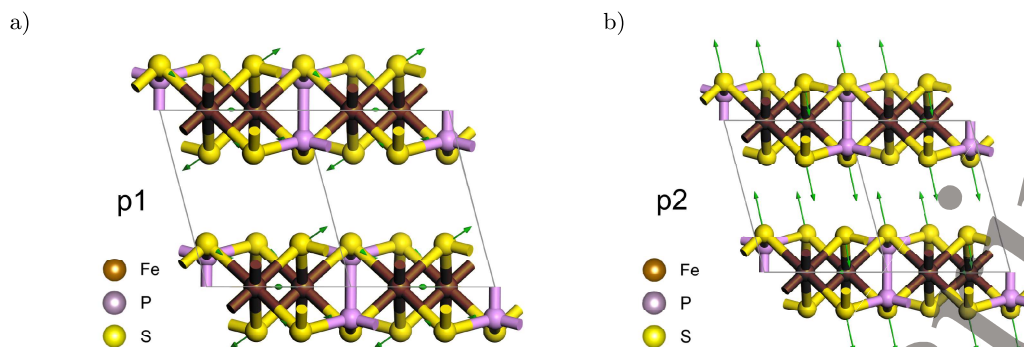


FIG. 7. Visualizations, looking along the  $ab$  planes with unit cell boundaries drawn in light grey, from calculation of Raman vibrational modes of  $V_{0.9}PS_3$  at 11 kbar. Mode p2 stands out as being an out-of-plane motion along the  $c^*$  axis - this mode alone is observed to stiffen at the insulator-metal transition.

### Methods

The magnetotransport data reported here on  $V_{0.9}PS_3$  and  $FePS_3$  were carried out in diamond anvil cells [60, 61] with non-magnetic BeCu bodies and BeCu and sintered diamond powder gaskets respectively. The cells were measured within a PPMS cryostat, Quantum Design, using the PPMS internal Resistivity measurement option. Single crystals were prepared in a 4-wire geometry in the  $ab$  plane, with gold contact pads evaporated onto freshly cleaved surfaces and gold wires bonded to these with DuPont 6838 silver-loaded epoxy. Glycerol was used as a pressure transmitting medium and the pressure was measured via the fluorescence spectrum of a chip of ruby placed within the pressure region [62]. Crystal structure visualisations were created in VESTA [63].

The authors would like to thank G.G. Lonzarich, P.A.C. Brown, S.E. Dutton, L.J. Spalek, Kaixuan Zhang, Junghyun Kim, Nahyun Lee and V. Tripathi for their generous help and discussions. This work was supported by the Institute for Basic Science (IBS) in Korea (Grant No. IBS-R009-G1). This work was carried out with the support of the Diamond Light Source and we acknowledge the provision of beamtime at I15 under proposal number NT21368. We thank H. Wilhelm for advice and help with the X-ray diffraction experiments at Diamond. We also acknowledge support from Jesus College of the University of Cambridge, the Engineering and Physical Sciences Research Council and the CHT Uzbekistan programme. The work was carried out with financial support from the Ministry of Education and Science of the Russian Federation in the framework of Increase Competitiveness Program of NUST MISiS (No. K2-2017-024). This project has received funding from the European Research Council (ERC) under the European Union's Horizon 2020 research and innovation programme (grant agreement No. 681260).

- [1] Park J-G 2016 Opportunities and challenges of 2D magnetic van der Waals materials: magnetic graphene? *J. Phys.: Cond. Matt.* **28**, 301001
- [2] Ajayan P, Kim P and Banerjee K 2016 Two-dimensional van der Waals materials *Physics Today* **69**, 38
- [3] Samarth N 2017 Condensed-matter physics: Magnetism in flatland *Nature* **546**, 216
- [4] Zhou Y, Lu H, Zu X and Gao F 2016 Evidencing the existence of exciting half-metallicity in two-dimensional  $TiCl_3$  and  $VCl_3$  sheets *Scientific Reports* **6**, 19407
- [5] Burch KS, Mandrus D and Park J-G 2018 Magnetism in two-dimensional van der Waals materials *Nature* **563**, 47
- [6] Manzeli S, Ovchinnikov D, Pasquier D, Yazyev OV, and Kis A 2017 2D transition metal dichalcogenides *Nature Reviews Materials* **2**, 17033
- [7] Friedel M 1894 *Bull. Soc. Chim. Fr.* **11**, 115
- [8] Friedel M 1894 *C.R. Acad. Sci.* **119**, 269
- [9] Klingen W, Eulenberger G and Hahn H 1968 Über Hexathio- und Hexaselenohypodiphosphate vom Typ  $M_2^{II}P_2X_6$  *Die Naturwissenschaften* **55**, 229
- [10] Klingen W 1969 Darstellung und Strukturbestimmung von Hexachalkogenohypodiphosphaten *Ph.D. thesis, Universität Hohenheim (LH)*
- [11] Klingen W, Eulenberger G and Hahn H 1970 Über Hexachalkogenohypodiphosphate vom Typ  $M_2P_2X_6$  *Naturwissenschaften* **57**, 88
- [12] Klingen W, Ott R and Hahn H 1973 Über die Darstellung und Eigenschaften von Hexathio- und Hexaselenohypodiphosphaten *Zeitschrift für anorganische und allgemeine Chemie* **396**, 271
- [13] Ouvrard G, Brec R and Rouxel J 1985 Structural determination of some  $MPS_3$  layered phases ( $M = Mn, Fe, Co, Ni$  and  $Cd$ ) *Materials Research Bulletin* **20**, 1181
- [14] Ouvrard G, Fréour R, Brec R and Rouxel J 1985 A mixed valence compound in the two dimensional  $MPS_3$  family:  $V_{0.78}PS_3$  structure and physical properties *Materials Research Bulletin* **20**, 1053
- [15] Grasso V and Silipigni L 2002 Low-dimensional materials: The  $MPX_3$  family, physical features and potential future applications *Rivista Del Nuovo Cimento* **25**,1
- [16] Brec R 1986 Review on structural and chemical properties of transition metal phosphorous trisulfides  $MPS_3$



- Solid State Ionics* **22**, 3
- [17] Chittari BL, Park Y, Lee D, Han M, MacDonald AH, Hwang E and Jung J 2016 Electronic and magnetic properties of single-layer  $\text{MPX}_3$  metal phosphorous trichalcogenides *Phys.Rev.B* **94**, 184428
- [18] Rabu P and Drillon M 2003 Layered Organic & Inorganic Materials: A Way towards Controllable Magnetism *Adv. Eng. Mater.* **5**, 189
- [19] Wang F, Shifa TA, Yu P, He P, Liu Y, Wang F, Wang Z, Zhan X, Lou X, Xia F and He J 2018 New Frontiers on van der Waals Layered Metal Phosphorous Trichalcogenides *Advanced Functional Materials* **28**, 1802151
- [20] Le Flem G, Brec R, Ouvard G, Louisy A and Segransan P 1982 Magnetic interactions in the layer compounds  $\text{MPX}_3$  (M= Mn, Fe, Ni; X= S, Se) *Journal of Physics and Chemistry of Solids* **43**, 455
- [21] Kurosawa K, Saito S and Yamaguchi Y 1983 Neutron Diffraction Study on  $\text{MnPS}_3$  and  $\text{FePS}_3$  *Journal of the Physical Society of Japan* **52**, 3919
- [22] Wildes AR, Kennedy SJ and Hicks TJ 1994 True two-dimensional magnetic ordering in  $\text{MnPS}_3$  *J. Phys.: Condens. Matter* **6**, L335
- [23] Wildes AR, Harris MJ and Godfrey KW 1998 Two-dimensional critical fluctuations in  $\text{MnPS}_3$  *Journal of Magnetism and Magnetic Materials* **177-181**, 143
- [24] Wildes AR, Roessli B, Lebeck B and Godfrey KW 1998 Spin waves and the critical behaviour of the magnetization in  $\text{MnPS}_3$  *J. Phys.: Condens. Matter* **10**, 6417
- [25] Rønnow HM, Wildes AR and Bramwell ST 2000 Magnetic correlations in the 2D honeycomb antiferromagnet  $\text{MnPS}_3$  *Physica B: Condensed Matter* **276-278**, 676
- [26] Rule KC, Kennedy SJ, Goossens DJ, Mulders AM and Hicks TJ 2002 Contrasting antiferromagnetic order between  $\text{FePS}_3$  and  $\text{MnPS}_3$  *Applied Physics A: Materials Science & Processing* **74**, s811
- [27] Rule KC, Ersez T, Kennedy SJ and Hicks TJ 2003 *Physica B: Condensed Matter* **335**, 6
- [28] Wildes AR, Rønnow H, Roessli B, Harris MJ and Godfrey KW 2006 Static and dynamic critical properties of the quasi-two-dimensional antiferromagnet  $\text{MnPS}_3$  *Phys. Rev. B* **74**, 094422
- [29] Rule KC, McIntyre GJ, Kennedy SJ and Hicks TJ 2007 Single-crystal and powder neutron diffraction experiments on  $\text{FePS}_3$ : Search for the magnetic structure *Phys. Rev. B* **76**, 134402
- [30] Wildes AR, Rønnow HM, Roessli B, Harris MJ and Godfrey KW 2007 Anisotropy and the critical behaviour of the quasi-2D antiferromagnet,  $\text{MnPS}_3$  *Journal of Magnetism and Magnetic Materials* **310**, 1221
- [31] Rule KC, Wildes AR, Bewley RI, Visser D and Hicks TJ 2009 High energy excitations measured by neutron spectroscopy in  $\text{FePS}_3$  *J. Phys.: Condens. Matter* **21**, 124214
- [32] Wildes AR, Rule KC, Bewley RI, Enderle M and Hicks TJ 2012 The magnon dynamics and spin exchange parameters of  $\text{FePS}_3$  *J. Phys.: Condens. Matter* **24**, 416004
- [33] Wildes AR, Simonet V, Ressouche E, McIntyre GJ, Avdeev M, Suard E, Kimber SAJ, Lançon D, Pepe G, Moubaraki B and Hicks TJ 2015 Magnetic structure of the quasi-two-dimensional antiferromagnet  $\text{NiPS}_3$  *Phys. Rev. B* **92**, 224408
- [34] Lançon D, Walker HC, Ressouche E, Ouladdiaf B, Rule KC, McIntyre GJ, Hicks TJ, Rønnow HM and Wildes AR 2016 Magnetic structure and magnon dynamics of the quasi-two-dimensional antiferromagnet  $\text{FePS}_3$  *Phys. Rev. B* **94**, 214407
- [35] Wildes AR, Simonet V, Ressouche E, Ballou R and McIntyre GJ 2017 The magnetic properties and structure of the quasi-two-dimensional antiferromagnet  $\text{CoPS}_3$  *J. Phys.: Condens. Matter* **29**, 455801
- [36] Maisonneuve V, Reau JM, Dong M, Cajipe VB, Payen C and Ravez J 1997 Ionic conductivity in ferroic  $\text{CuInP}_2\text{S}_6$  and  $\text{CuCrP}_2\text{S}_6$  *Ferroelectrics* **196**, 257
- [37] Maisonneuve V, Cajipe VB, Simon A, Von Der Muhll R and Ravez J 1997 Ferroelectric ordering in lamellar  $\text{CuInP}_2\text{S}_6$  *Phys.Rev.B* **56**, 10860
- [38] Guranich P, Shusta V, Gerzanich E, Slivka A, Kuritsa I and Gomonnai O 2007 Influence of hydrostatic pressure on the dielectric properties of  $\text{CuInP}_2\text{S}_6$  and  $\text{CuInP}_2\text{Se}_6$  layered crystals *Journal of Physics: Conference Series* **79**, 012009
- [39] Belianinov A, He Q, Dziazugys A, Maksymovych P, Eliseev E, Borisevich A, Morozovska A, Banys J, Vysochanskii Y and Kalinin SV 2015  $\text{CuInP}_2\text{S}_6$  Room Temperature Layered Ferroelectric *Nano Letters* **15**, 3808
- [40] Takano Y, Arai A, Takahashi Y, Takase K and Sekizawa K 2003 Magnetic properties and specific heat of new spin glass  $\text{Mn}_{0.5}\text{Fe}_{0.5}\text{PS}_3$  *Journal of Applied Physics* **93**, 8197
- [41] Masubuchi T, Hoya H, Watanabe T, Takahashi Y, Ban S, Ohkubo N, Takase, K and Takano Y 2008 Phase diagram, magnetic properties and specific heat of  $\text{Mn}_{1-x}\text{Fe}_x\text{PS}_3$  *Journal of Alloys and Compounds* **460**, 668
- [42] Ressouche E, Loire M, Simonet V, Ballou R, Stunault A and Wildes AR 2010 Magnetolectric  $\text{MnPS}_3$  as a candidate for ferrotoroidicity *Phys.Rev.B* **82**, 100408
- [43] Du KZ, Wang XZ, Liu Y, Hu P, Utama MIB, Gan CK, Xiong Q and Kloc C 2016 Weak Van der Waals Stacking, Wide-Range Band Gap, and Raman Study on Ultrathin Layers of Metal Phosphorus Trichalcogenides *ACS Nano* **10**, 1738
- [44] Kuo CT, Neumann M, Balamurugan K, Park HJ, Kang S, Shiu HW, Kang JH, Hong BH, Han MS, Noh, TW and Park J-G 2016 Exfoliation and Raman Spectroscopic Fingerprint of Few-Layer  $\text{NiPS}_3$  Van der Waals Crystals *Scientific Reports* **6**, 20904
- [45] Wang Y, Ying J, Zhou Z, Sun J, Wen T, Zhou Y, Li N, Zhang Q, Han F, Xiao Y, Chow P, Yang W, Struzhkin VV, Zhao Y, and Mao H-K 2018 Emergent superconductivity in an iron-based honeycomb lattice initiated by pressure-driven spin-crossover *Nat. Comms* **9**, 1914
- [46] Novoselov KS, Geim AK, Morozov SV, Jiang D, Zhang Y, Dubonos SV, Grigorieva IV and Firsov AA 2004 Electric Field Effect in Atomically Thin Carbon Films *Science* **306**, 666
- [47] Lee JU, Lee SM, Ryoo JH, Kang SM, Kim TY, Kim PW, Park CH, Park J-G and Cheong HS 2016 Ising-Type Magnetic Ordering in Atomically Thin  $\text{FePS}_3$  *Nano Letters* **16**, 7433
- [48] Kim KW, Lim SY, Lee J-U, Lee SM, Kim TY, Park KS, Jeon GS, Park C-H, Park J-G and Cheong HS 2019 Suppression of magnetic ordering in XXZ-type antiferromagnetic monolayer  $\text{NiPS}_3$  *Nat Comms* **10**, 345
- [49] Kim K, Lim SY, Kim J, Lee J-U, Lee S, Kim P, Park K, Son S, Park C-H, Park J-G and Cheong HS 2019 Antiferromagnetic ordering in van der Waals two-dimensional magnetic material  $\text{MnPS}_3$  probed by Raman spectroscopy *2D Materials* **6**

- 1  
2  
3  
4  
5  
6  
7  
8  
9  
10  
11  
12  
13  
14  
15  
16  
17  
18  
19  
20  
21  
22  
23  
24  
25  
26  
27  
28  
29  
30  
31  
32  
33  
34  
35  
36  
37  
38  
39  
40  
41  
42  
43  
44  
45  
46  
47  
48  
49  
50  
51  
52  
53  
54  
55  
56  
57  
58  
59  
60
- [50] Tien DH, Park J-Y, Kim KB, Lee N, Choi T, Kim P, Taniguchi T, Watanabe K and Seo Y 2016 Study of Graphene-based 2D-Heterostructure Device Fabricated by All-Dry Transfer Process *ACS Applied Materials & Interfaces* **8**, 3072
- [51] Haines CRS, Coak MJ, Wildes AR, Lampronti GI, Liu C, Nahai-Williamson P, Hamidov H, Daisenberger D and Saxena SS 2018 Pressure-Induced Electronic and Structural Phase Evolution in the van der Waals Compound FePS<sub>3</sub> *Phys. Rev. Lett.* **121**, 266801
- [52] Coak MJ, Son S, Daisenberger D, Hamidov H, Haines CRS, Alireza PL, Wildes AR, Cheng Liu C, Saxena SS and Park J-G 2019 *npj Quantum Materials* **4**, 38
- [53] Jarvis DM, Hamidov H, Coak MJ, Haines CRS, Wildes AR, Liu C, Daisenberger D and Saxena SS 2019 *In preparation*
- [54] Coak MJ, Kim Y-H, Yi YS, Son S, Lee SK and Park J-G 2019 Electronic and vibrational properties of the two-dimensional Mott insulator V<sub>0.9</sub>PS<sub>3</sub> under pressure *Phys. Rev. B* **100**, 035120
- [55] Wang Y, Zhou Z, Wen T, Zhou Y, Li N, Han F, Xiao Y, Chow P, Sun J, Pravica M, Cornelius AL, Yang W and Zhao Y 2016 Pressure-Driven Cooperative Spin-Crossover, Large-Volume Collapse, and Semiconductor-to-Metal Transition in Manganese(II) Honeycomb Lattices *Journal of the American Chemical Society* **138**, 15751
- [56] Lifshitz E, Francis AH and Clarke R 1983 An ESR and X-ray diffraction study of a first-order phase transition in CdPS<sub>3</sub> *Solid State Communications* **45**, 273
- [57] Boucher F, Evain M and Brec R 1995 Phase transition upon d10 Cd<sup>2+</sup> ordering in CdPS<sub>3</sub> *Acta Crystallogr Sect B Struct Sci* **51**, 952
- [58] Haines CRS 2011 Pressure Tuned Magnetism in d and f Electron Materials *Ph.D. thesis, University of Cambridge*
- [59] Nahai-Williamson P 2011 Tuning ordered states in transition metal chalcogenide systems *Ph.D. thesis, University of Cambridge*
- [60] Dunstan DJ and Spain IL 1989 Technology of diamond anvil high-pressure cells: I. Principles, design and construction *J. Phys. E: Sci. Instrum.* **22**, 913
- [61] Spain IL and Dunstan DJ 1989 The technology of diamond anvil high-pressure cells: II. Operation and use *J. Phys. E: Sci. Instrum.* **22**, 923
- [62] Mao HK, Xu J and Bell PM 1986 Calibration of the ruby pressure gauge to 800 kbar under quasi-hydrostatic conditions *Journal of Geophysical Research* **91**, 4673
- [63] Momma K and Izumi F 2011 VESTA 3 for three-dimensional visualization of crystal, volumetric and morphology data *J Appl Cryst* **44**, 1272